Digital microfluidics for cell-based assays

Irena Barbulovic-Nad,[a,b] Hao Yang,[c] Philip S. Park[c] and Aaron R. Wheeler*[a,b,c]

Received 19th November 2007, Accepted 24th January 2008
First published as an Advance Article on the web 25th February 2008
DOI: 10.1039/b717759c

We introduce a new method for implementing cell-based assays. The method is based on digital microfluidics (DMF) which is used to actuate nanolitre droplets of reagents and cells on a planar array of electrodes. We demonstrate that this method is advantageous for cell-based assays because of automated manipulation of multiple reagents in addition to reduced reagent use and analysis time. No adverse effects of actuation by DMF were observed in assays for cell viability, proliferation, and biochemistry. A cytotoxicity assay using Jurkat T-cells was performed using the new method, which had ~ 20 times higher sensitivity than a conventional well plate assay. These results suggest that DMF has great potential as a simple yet versatile analytical tool for implementing cell-based assays on the microscale.

Introduction

The cell is the irreducible element of life and is often studied as a living model of complex biological systems. Cell-based assays are conventionally performed in well plates that enable simultaneous analysis of multiple cell types or stimuli. For such multiplexed analyses, cells in well plates are often evaluated using microplate readers, which can be integrated with fluid handling and other miscellaneous equipment in a robotic analysis platform. A major drawback of such systems is the expense of the instrumentation and the experimental consumables (*e.g.*, plates, pipette tips, reagents, and cells). The latter is a particular disadvantage for cell-based assays as they are generally more complex and require larger amounts of reagents than cell-free assays.[1]

Recently, microfluidics has been touted as a solution for the challenges inherent in conducting multiplexed cell-based assays.[2] The conventional format for microfluidics, which is characterized by devices containing networks of micron-dimension channels, allows integration of multiple processes on a single platform while reducing reagent consumption and analysis time. There are numerous advantages of using microfluidic based systems for cell assays, some of which are similarity in dimensions of cells and microchannels (10–100 μm widths and depths), laminar flow dominance and formation of highly resolved chemical gradients,[3,4] subcellular delivery of stimuli,[5] reduced dilution of analytes, and favorable scaling of electrical and magnetic fields. For the last ten years, researchers have used microchannels to manipulate and sort cells,[6,7] to analyze cell lysates,[8–10] to assay intact-cell biochemistry,[11–13] and to evaluate cell mechanical[14,15] and electrical[16,17] responses. In most of these studies, cells were exposed to one stimulus or to a limited number of stimuli. There have been just a few attempts to conduct multiplexed assays[18–21] as it is difficult to control many reagents simultaneously in a complex network of connected channels, even when using microvalve architectures developed for microfluidic devices.[22,23] Finally, we note that there have been only a few microfluidic devices integrated to multiplexed detection instruments such as microplate readers;[24] we believe this will be a necessary step for the technology to become competitive with robotic screening systems.

A potential solution to the limitations of the channel-microfluidic format is the use of "digital" or droplet-based microfluidics. In digital microfluidics (DMF), discrete droplets containing reagents are manipulated by applying potentials between electrodes in an array. As described elsewhere, droplets are actuated by electrowetting[25,26] (Laplace forces generated by non-symmetric contact angles), and/or dielectrophoresis[27–29] (attractive or repulsive forces caused by polarization effects in non-uniform electric fields). Droplets can be manipulated independently or in parallel on a reconfigurable path defined by the electrode actuation sequence, which allows for precise spatial and temporal control over reagents. As with all microscale techniques, cross-contamination is a concern for DMF, but this phenomenon can be avoided by dedicating separate paths for each reagent. DMF has been used to actuate a wide range of volumes (nL to μL) and, unlike channel devices, there is no sample wasted in creating small plugs for analysis. In addition, each droplet is isolated from its surroundings rather than being embedded in a stream of fluid—a simple method of forming a microreactor in which there is no possibility that products will diffuse away.

There is currently much enthusiasm for using DMF to implement multiplexed assays;[30] however, it has only been applied to a few applications, including on-chip enzyme assays,[31–35] preparation of protein samples for analysis by matrix assisted laser desorption/ionization mass spectrometry (MALDI-MS),[36–38] and nanolitre-scale PCR.[39] To our knowledge, there are no reports of the use of DMF to analyze cells, other than a

[a]*Institute for Biomaterials and Biomedical Engineering, University of Toronto, 164 College St., Toronto, ON, M5S 3G9, Canada. E-mail: awheeler@chem.utoronto.ca; Fax: +1 (416) 946 3865; Tel: +1 (416) 946 3864*
[b]*Donnelly Centre for Cellular and Biomolecular Research, 160 College St., Toronto, ON, M5S 3E1, Canada*
[c]*Department of Chemistry, University of Toronto, 80 St George St., Toronto, ON, M5S 3H6, Canada*

conference paper describing a cell-concentration application.[40] This is surprising, as cell-based assays seems a natural fit for the technique—in addition to the potential for multiplexed analysis, DMF is likely to facilitate cell-based assays under static fluid/media conditions, avoiding unwanted shear stress.

Here, we demonstrate the first application of digital microfluidic methods to the manipulation and analysis of cells. We show that the effects of actuation by DMF on cell vitality are minimal, and in addition, we show that a cytotoxicity assay implemented by DMF has much better sensitivity than macroscale methods, which suggests applications in regulatory policy and in drug discovery. We also demonstrate compatibility of DMF cell assays with fluorescence microplate reader detection. This technique has great potential as a simple yet versatile analytical tool for implementing cell-based assays on the microscale.

Experimental

Reagents and materials

Unless otherwise indicated, reagents used outside of the clean room were purchased from Sigma-Aldrich (Oakville, ON), and cells and cell culture reagents were from American Type Culture Collection (ATCC, Manassas, VA). Fluorescent dyes were from Invitrogen-Molecular Probes (Eugene, OR), Parylene-C dimer was from Specialty Coating Systems (Indianapolis, IN), and Teflon-AF was purchased from DuPont (Wilmington, DE). Clean room reagents and supplies included Shipley S1811 photoresist and MF-321 developer from Rohm and Haas (Marlborough, MA), solid chromium and gold from Kurt J. Lesker Canada (Toronto, ON), standard gold etchant from Sigma-Aldrich, CR-4 chromium etchant from Cyantek (Fremont, CA), AZ-300T photoresist striper from AZ Electronic Materials (Somerville, NJ), and hexamethyldisilazane (HMDS) from Shin-Etsu MicroSi (Phoenix, AZ). Concentrated sulfuric acid and hydrogen peroxide (30%) were from Fisher Scientific Canada (Ottawa, ON), and piranha solution was prepared as a 3 : 1 (v/v) mixture of sulfuric acid and hydrogen peroxide.

Cell culture

Jurkat T-cells (human leukemia lymphocytes) were maintained in a humidified atmosphere (5% CO_2, 37 °C) in RPMI 1640 medium supplemented with 10% fetal bovine serum (Invitrogen Canada, Burlington, ON), penicillin (100 IU mL^{-1}), and streptomycin (100 μg mL^{-1}). Cells were subcultured every 3–4 days at ~1×10^6 cells mL^{-1}. A working buffer of 0.2% (wt/v) pluronic F68 (Sigma-Aldrich) in Dulbecco's phosphate buffered saline (PBS) (Invitrogen Canada) was used for most cell-based assays. Prior to experiments, cells were washed three times in PBS, suspended in 0.2% F68 (wt/v) in PBS at 3.5×10^6 cells mL^{-1}, and then incubated at room temperature (1 h). Cell numbers and viability were quantified using a hemocytometer and trypan blue exclusion (Invitrogen Canada) immediately prior to all experiments. Prior to cell viability/proliferation assays and analysis by mass spectrometry, cells were incubated for 1 h in 3% (wt/v) F68 in PBS at 7.2×10^6 cells mL^{-1} and at 6×10^7 cells mL^{-1}, respectively.

Device fabrication and use

Digital microfluidic devices were fabricated using conventional methods in the University of Toronto Emerging Communications Technology Institute (ECTI) cleanroom facility, using chrome-on-glass photomasks printed at the UCLA Nanofabrication facility (Los Angeles, CA). Glass wafers (Howard Glass Co. Inc., Worcester, MA) were cleaned in piranha solution (10 min), and then coated with chromium (10 nm) and gold (100 nm) by electron beam deposition. After rinsing and drying, the substrates were primed by spin-coating with HMDS (3000 rpm, 30 s) and then spin-coating again with Shipley S1811 photoresist (3000 rpm, 30 s). Substrates were pre-baked on a hotplate (100 °C, 2 min), and then exposed to UV radiation (35.5 mW cm^{-2}, 365 nm, 4 s) through a photomask using a Karl Suss MA6 mask aligner (Garching, Germany). After exposure, substrates were developed in MF-321 (3 min), and then post-baked on a hot plate (100 °C, 1 min). Following photolithography, substrates were immersed in gold etchant (40 s) followed by chromium etchant (30 s). The remaining photoresist was stripped in AZ-300T (10 min).

After forming electrodes and cleaning in piranha solution (30 s), substrates were coated with 2 μm of Parylene-C and 50 nm of Teflon-AF. Parylene-C was applied using a vapor deposition instrument (Specialty Coating Systems), and Teflon-AF was spin-coated (1% wt/wt in Fluorinert FC-40, 2000 rpm, 60 s) followed by post-baking on a hot-plate (160 °C, 10 min). The polymer coatings were removed from contact pads by gentle scraping with a scalpel to facilitate electrical contact for droplet actuation. In addition to patterned devices, unpatterned indium-tin oxide (ITO) coated glass substrates (Delta Technologies Ltd, Stillwater, MN) were coated with Teflon-AF (50 nm, as above).

Devices were assembled with an unpatterned ITO–glass top plate and a patterned bottom plate separated by a spacer formed from two pieces of double-sided tape (~150 μm thick). Driving potentials (100–140 V_{RMS}) were generated by amplifying the output of a function generator (Agilent Technologies, Santa Clara, CA) operating at 15 kHz. Droplets were sandwiched between the two plates and actuated by applying driving potentials between the top electrode (ground) and sequential electrodes on the bottom plate (Fig. 1(b)) *via* the exposed contact pads. Droplet actuation was monitored and recorded by a CCD camera mated to a stereomicroscope with fluorescence imaging capability (Olympus Canada, Markham, ON). Most devices used here had a geometry identical to that shown in Fig. 1(a), with 1 mm × 1 mm actuation electrodes (suitable for manipulating 150 nL droplets), and inter-electrode gaps of 5–40 μm. Some devices had 7 mm × 7 mm actuation electrodes which were used to manipulate much larger droplets (11 μL).

Electrical field modeling

Electrical fields in digital microfluidic devices were modeled with COMSOL Multiphysics 3.3a (COMSOL, Burlington, MA) using the conductive media direct current module and the electrostatics module. The two-dimensional geometry of the model was nearly identical to the device illustrated in Fig. 1(b), including three patterned electrodes (1 mm length) on the bottom plate, a layer of parylene (2 μm thick), a layer of PBS

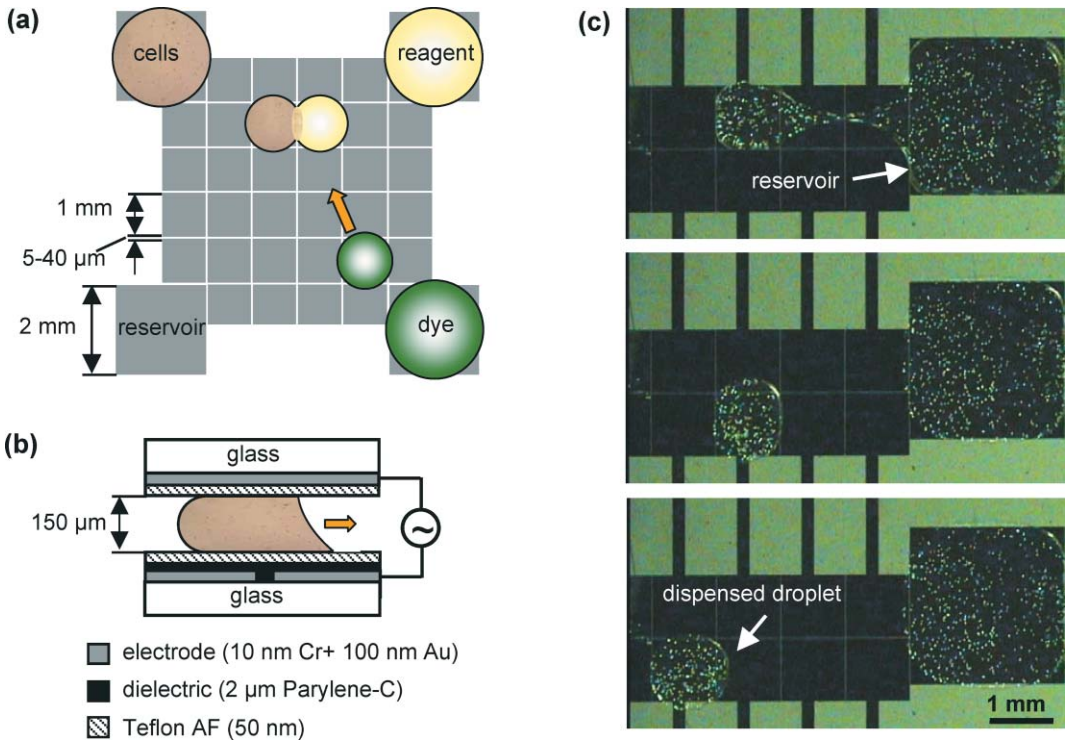

Fig. 1 Schematics (a) and (b) and sequence of pictures from a movie (top-to-bottom) (c) of DMF devices used for cell-based assays. The top view schematic (a) depicts a complete device, while the side view schematic (b) shows only two actuation electrodes. In (c), a 150 nL droplet containing ~260 cells is dispensed from a reservoir on a device with identical dimensions but fewer electrodes than the design shown in (a). Cells were labeled with calcein AM, which fluoresces green.

and air (150 μm thick), and a continuous electrode on the top plate. The Teflon AF layer was omitted from the model because of its porosity and insignificant thickness. Dielectric constants, ε, and conductivities, σ, used in the model included $\varepsilon_{parylene} = 2.65$, $\varepsilon_{pbs} = 70$, $\varepsilon_{air} = 1$, $\sigma_{parylene} = 0$ S m^{-1}, $\sigma_{air} = 0$ S m^{-1}, and $\sigma_{pbs} = 4.7$ S m^{-1} (measured using a conductivity meter). With a 100 V potential applied between the bottom-right electrode and the top electrode (ground), a mesh with 233 831 triangular elements was used to simulate electrical field, using the linear solver UMFPACK.

Vitality assays

The effects of the electric field driven droplet actuation on cell vitality were evaluated by three assays, measuring cell viability, proliferation, and biochemistry. In these assays, large droplets (>1 μL) were used because the more conventional sub-microlitre droplets (used in the cell phenotype assays) were difficult to handle off-chip and did not contain enough cells for analysis. In the cell viability and proliferation assays, ten 11 μL droplets of cells suspended in PBS/F68 (each containing ~79 200 cells) were actuated on devices with 7 × 7 mm electrodes. Each droplet was moved across 10 electrodes (approximately 15 s of actuation per droplet) and was then removed from the device and suspended in 300 μL of cell medium at 2.5×10^5 cells mL^{-1}. For viability assays, immediately after suspension in media, live and dead cells were counted on a hemacytometer with trypan blue exclusion. For proliferation assays, live and dead cells were counted after 48 h of incubation off-chip (humidified incubator, 5% CO_2, 37 °C). A second group of ten 11 μL droplets of the original cell solution (in PBS/F68) were treated identically, but were not actuated, and served as a control. The data was analyzed with two-tailed t-tests assuming unequal variances.

In the cell biochemistry assay, four 11 μL droplets of cell suspension (~6.6×10^5 cells droplet^{-1}) were actuated over ten electrodes as above, and were then pooled and suspended in lysing medium at 3×10^7 cells mL^{-1}. Lysing medium was PBS with 3% (wt/v) F68, 1% Triton X-100, and 1 mM phenylmethylsulfonyl fluoride (PMSF). After incubation on ice (30 min), the lysate was centrifuged (12 000 rpm, 5 min) and the supernatant was collected and stored in a −85 °C freezer. Immediately prior to analysis, the supernatant (100 μL) was thawed and desalted using a microspin G-25 column (Amersham BioSciences, Piscataway, NJ) at 2800 rpm for 2 min. Proteins were eluted in distilled water with 0.05% (v/v) Kathon (1.5 μL), and the eluent was spotted onto a MALDI (matrix assisted laser desorption/ionization) target plate. A 1.5 μL aliquot of MALDI matrix solution (10 mg mL^{-1} sinapinic acid in 80% (v/v) acetonitrile/water) was added and the combined droplet was allowed to dry. Non-actuated droplets of the original cell suspension were lysed and processed identically, and served as a control.

Samples were analyzed using a MALDI-TOF Micro MX mass spectrometer (Waters, Milford, MA) in linear positive mode for the mass range of 4 000 to 25 000 m/z. One hundred shots were collected per spectrum, with laser power tuned to optimize the signal to noise ratio. Data were then processed

by normalization to the largest analyte peak and baseline subtraction and were smoothed with a 15-point running average.

Cell phenotype assays

For phenotypic assays, cells were exposed to the surfactant, Tween 20 (lethal to mammalian cells at high concentrations), diluted in working buffer in a range of concentrations (0.002% to 0.5% (wt/v)). Each Tween 20 concentration was evaluated in 4–6 replicates. In each experiment, a 150 nL droplet containing ~525 cells was dispensed and merged with a 150 nL droplet containing Tween 20. The merged droplets were then actively mixed by moving them on four neighboring electrodes in a circle. After 20 min of incubation in a humidified environment (a closed Petri dish half-filled with water), the combined droplet containing cells and Tween 20 was merged and mixed with a 150 nL probe droplet containing viability dye(s), and then incubated for a second time in a humidified environment (20 min). In all experiments, the probe droplet contained calcein AM (1 μM in the working buffer), and in some experiments, the droplet also contained ethidium homodimer-1 (2 μM in the working buffer).

For quantitative experiments, a digital microfluidic device was positioned on the top of a well plate and inserted into a fluorescence microplate reader (Pherastar, BMG Labtech, Durham, NC) equipped with a module for 480 nm excitation and 520 nm emission. Each droplet was evaluated using a multipoint scanning program, in which the average fluorescence was recorded from each of 9 excitation flashes illuminated onto a 1 mm square 3 × 3 array with 0.5 mm resolution. The array was located in the centre of each droplet, and the focal height was set for each analysis at the highest-signal intensity, with gain = 376. This multipoint program, designed by BMG Labtech for standard assays in well plates, was found empirically to have lower variance between runs than comparable single point analyses. Samples containing only Tween-20, pluronic F68, and calcein AM in PBS were evaluated to determine the background signal. Each analysis was repeated 4–6 times to determine standard deviations. All data were normalized to the average fluorescence intensity of cell samples exposed to control droplets (containing no Tween-20), and were plotted as a function of Tween-20 concentration.

For comparison, each assay implemented by digital microfluidics was duplicated in standard 384-well plates by pipetting reagents, cells, and dyes. In these experiments, all parameters were identical to those described above, except that the ~525 cells, reagents, and dyes were suspended in a final volume of 15 μL.

Results and discussion

Cell manipulation by DMF

While digital microfluidics has been used previously to manipulate and evaluate a wide range of liquids and reagents,[41] we report here the first application of digital microfluidics to transport and analyze biological cells. Using the parameters reported in the experimental section, cell suspensions representing a wide range of concentrations (including very dense solutions of 6×10^7 cells mL^{-1}) were found to be feasible to actuate by DMF, with no differences observed in velocity or reliability relative to liquids not containing cells. For example, Fig. 1(c) depicts a routine operation in our experiments: dispensing of a 150 nL droplet containing ~260 Jurkat T-cells (the cells are stained with calcein AM, which fluoresces green). However, in initial work (with un-optimized parameters), droplets containing cells were difficult to manipulate, as cells tended to stick to the surface of the devices, causing contact line pinning.[42] This problem was overcome by the use of the non-ionic surfactant, pluronic F68, which when used as a solution additive, facilitated actuation of suspensions of cells in all liquids tested (including PBS and complete media containing 10% fetal bovine serum).

Pluronics are block copolymers formed from poly(propylene oxide) (PPO) and poly(ethylene oxide) (PEO), and are commonly used as surface coatings for preventing non-specific protein adsorption.[10,43] In our work, we used pluronics in solution, rather than as a surface coating; we hypothesize that in this configuration, the polymer coats cells and proteins in a manner such that their functionality is retained, but adsorption to hydrophobic surfaces is minimized. We note that pluronic F68 has been used extensively in cell-based assays with no evidence for detrimental effects on cell vitality,[44,45] and it is even used as a constituent in commercial cell growth media.[46] Our experiments support this trend—Jurkat T-cells incubated in medium containing 0.2% (wt/v) F68 for 4 days (humidified incubator, 5% CO_2, 37 °C) had identical growth rates and morphology as cells grown in media without pluronics. In ongoing work, the optimal conditions (concentration and type of pluronic, *etc.*) for reducing unwanted adsorption in DMF are being evaluated;[47] we used F68 for all of the results reported here.

A second challenge for using DMF for actuation of cells is droplet evaporation, which raises the concentration of salts and other buffer constituents, making the solution hypertonic. In the work described here, we controlled evaporation by positioning devices in a humidified atmosphere when not actively manipulating droplets by DMF. For the duration of our experiments (up to a few hours), such measures prevented significant evaporation, and no negative effects on cell viability were observed. In current work, we are developing a customized, sterile, humidified chamber that will contain DMF devices for the full duration of an experiment (including actuation, incubation, and analysis)—we expect this apparatus will facilitate long-term cell culture and examination. But irrespective of future work, the measures described here were sufficient for implementing cell-based assays (described below).

Effects of DMF manipulation on cell vitality

Digital microfluidic devices use electrical fields to actuate droplets, which led us to investigate the effects of droplet actuation on cell vitality. As described above, droplets were sandwiched between an energized electrode on a bottom plate and a ground electrode on a top plate (Fig. 1(b)). Because of the high conductivity of a droplet of PBS relative to the insulating layer formed from Parylene-C, we hypothesized that cells would experience negligible electrical field upon application of driving potentials. This hypothesis was supported by a numerical simulation using the COMSOL Multiphysics 3.3a analysis package. In a simulation in which 100 V was applied

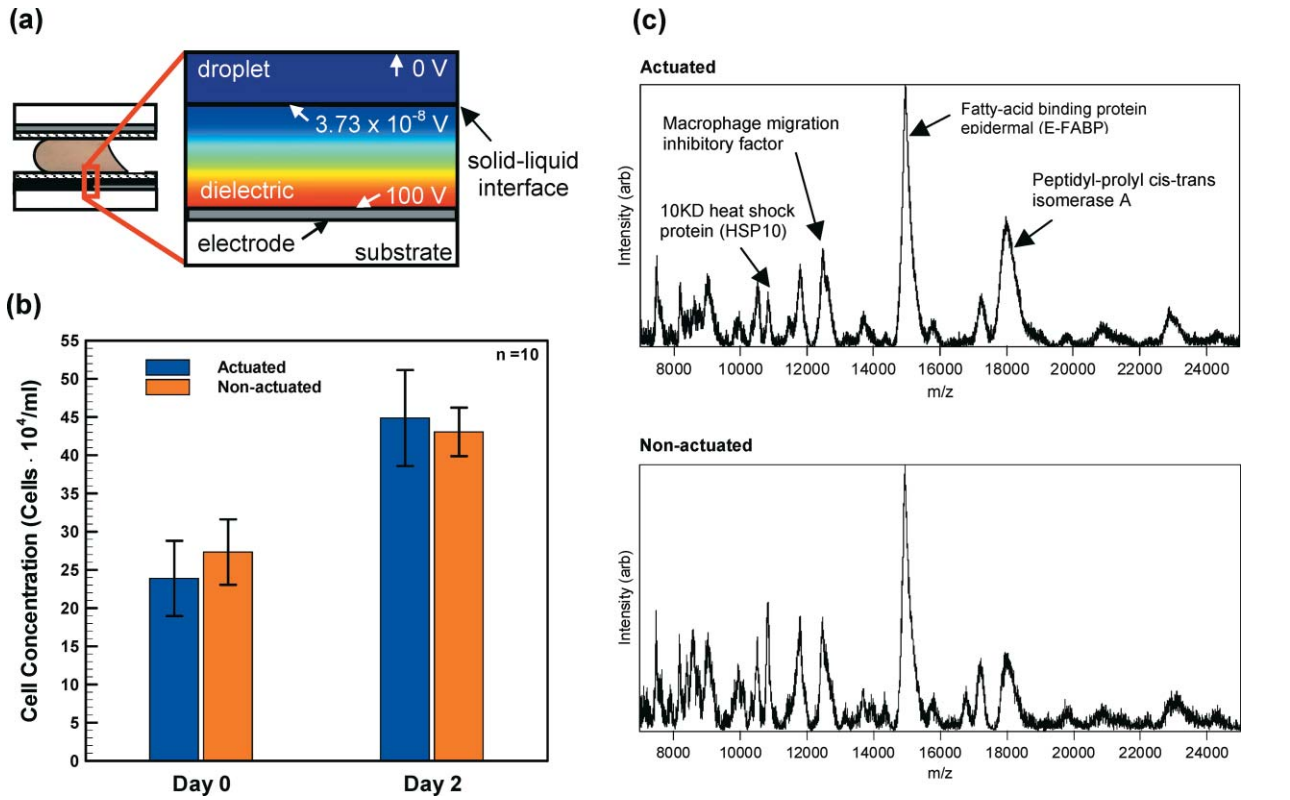

Fig. 2 Numerical simulation of the distribution of electrical potentials (a) and results of vitality tests (b–c) for cells actuated by digital microfluidics. For (a), the right panel was generated by a COMSOL Multiphysics 3.3a simulation of the potential drops across a droplet and a dielectric layer; potentials are plotted as a heat map, ranging from red (100 V) to blue (0 V). In the simulation, the top electrode was held at 0 V, and the bottom electrode at 100 V. According to the simulation, 3.73×10^{-8} V drops across the droplet of PBS. In (b), droplets were actuated across 10 electrodes and then suspended in media at 2.5×10^5 cells mL^{-1}. Non-actuated cells were also suspended in media at the same concentration. Cells in both groups were counted with trypan blue exclusion after actuation (Day 0) and after 48 h incubation in a humidified atmosphere (Day 2). No significant differences were found between the groups for either assay ($P = 0.11$ for the viability assay, $P = 0.43$ for the proliferation assay). Each point represents 10 replicates, and error bars are 1 SD. In (c), cells in droplets were actuated, lysed, and analyzed by MALDI-MS. As shown, there were no major qualitative differences between the actuated and non-actuated cells.

between top and bottom electrodes, the potential drop in the droplet was found to be only 3.73×10^{-8} V, or 0.00000004% of the applied potential (Fig. 2(a)). Thus, we would expect to observe modest effects (if any) on the vitality of suspensions of cells, upon application of electrical field. These effects were evaluated by three tests, measuring cell viability, proliferation, and biochemistry.

The viability of actuated and non-actuated cells was compared immediately after actuation, and proliferation was measured after 48 h incubation in a humidified incubator. As Fig. 2(b) illustrates, there was no significant difference between actuated and non-actuated cells ($P = 0.11$ for the viability assay, $P = 0.43$ for the proliferation assay). Cell biochemistry was evaluated qualitatively by analyzing lysates with MALDI mass spectrometry. Spectra of lysates of actuated and non-actuated cells are shown in Fig. 2(c). From previous studies of protein content in Jurkat T-cells,[48] we tentatively assigned several peaks, including heat shock protein (HSP10), macrophage migration inhibitory factor, epidermal fatty-acid binding protein (E-FABP), and peptidyl-prolyl *cis–trans* isomerase A. As shown, there are no major qualitative differences between the two spectra, which suggests that actuation by DMF does not have catastrophic effects on cell biochemistry. We note that MALDI-MS is not a quantitative analysis technique (*i.e.*, peak heights can vary considerably within multiple spectra of a single sample), and in on-going work, we plan to evaluate the gene expression of T-cells and other cell types using quantitative PCR. Regardless of future analyses, the results of these initial viability, proliferation, and biochemistry assays suggests that DMF actuation does not significantly alter cell vitality.

Cell phenotype assays by DMF

To illustrate that DMF is compatible with phenotypic assays, a dose–response toxicology screen was performed using Jurkat T-cells. Cells were exposed to varying concentrations of the surfactant, Tween 20 (0.002% to 0.5% (v/v)) (Fig. 3(a)) and then stained with viability dyes (Fig. 3(b)). The complete assay, from droplet dispensing to the final incubation with dyes was performed on-chip. 150 nL droplets (~1 mm in diameter) were dispensed *via* DMF, and after merging and incubation, resulted in a final ~450 nL droplet (~1.8 mm diameter, 150 μm height). An equivalent assay was implemented in a 384-well plate with the same number of cells (~525 cells/well or droplet) but different sample volume. In the well plate assays, 5 μL aliquots of each reagent were pipetted into conical wells (3.3 mm top, 2 mm

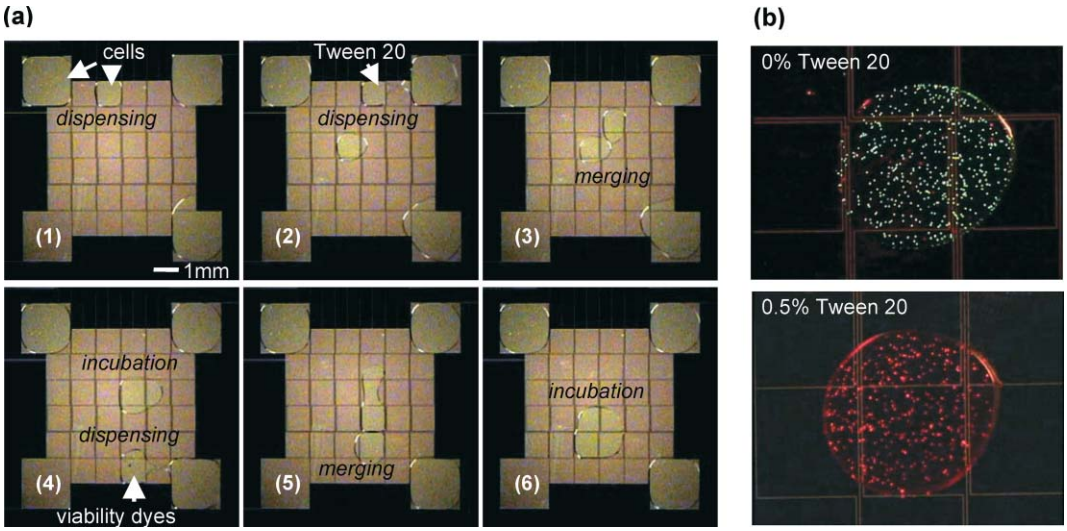

Fig. 3 Images from a movie depicting a DMF cell-based assay. In (a), a 150 nL droplet containing ~525 cells was dispensed (1) and merged with a 150 nL droplet of Tween 20 dispensed from a second reservoir (2, 3). The merged droplet was actively mixed on four neighboring electrodes. After 20 min incubation in a humidified environment, the combined droplet was merged and mixed with a 150 nL droplet containing viability dyes (4, 5). The final droplet was incubated 20 min in a humidified environment (6). (b) Fluorescent images of droplets treated with 0% (top) and 0.5% (bottom) Tween 20. Calcein AM (green) stains live cells, and ethidium homodimer-1 (red) stains dead cells. In the former droplet, almost all cells were live, and in the latter, all cells were dead.

bottom diameter) resulting in a final volume of 15 μL (~5 mm height) which is in the recommended range for 384-well plates. Hence, well plates required ~30-fold greater reagent use than DMF, leading to a much lower cell concentration in the wells. As described below, this had significant effects on assay sensitivity.

A fluorescence plate reader was used to generate dose–response curves for DMF and well plate assays using identical settings. As shown in Fig. 4, the DMF assays had much lower background signals, resulting in a much larger signal-to-noise ratio than the well-based assays. As a consequence, the lowest detectable number of live cells in droplets was ~10, compared to ~200 cells in wells. The latter value matches the general limits of detection listed by the manufacturer for such assays. One consequence of this difference was the determination of different 100%-lethal concentrations of Tween 20: ~0.5% (v/v) from the DMF assay and ~0.03% (v/v) from the well plate assay. The true 100%-lethal concentration was determined empirically by staining cells exposed to varying concentrations of Tween-20 and counting them using a hemacytometer. At the concentrations evaluated here, the fluorescence plate reader results generated by the digital microfluidic method were found to be a much better approximation of the empirical value than the conventional method. Thus, in this assay, the conventional method overestimates the toxicity of Tween 20 by more than

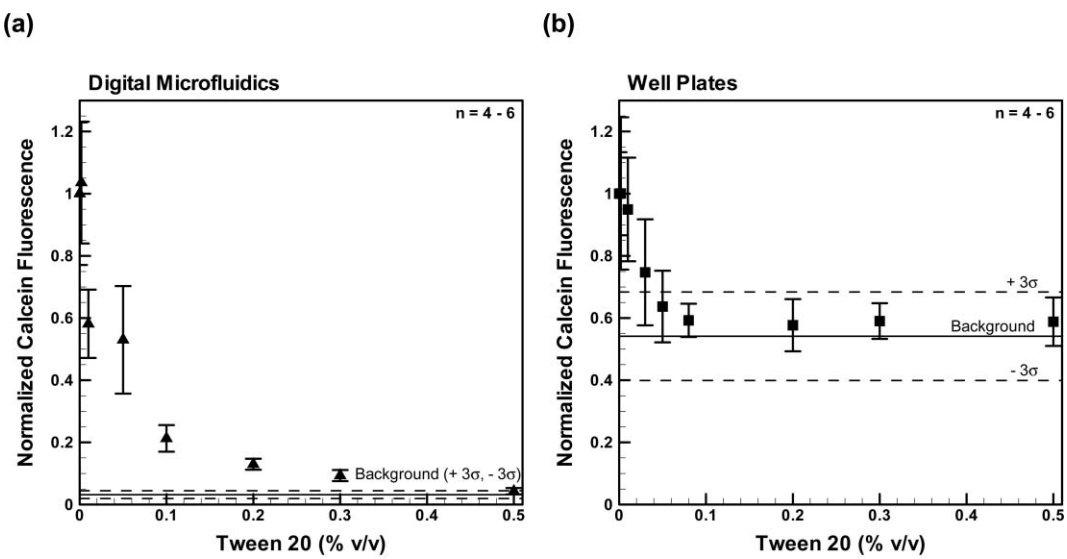

Fig. 4 Dose–response curves for Jurkat T-cells exposed to Tween 20 (0.002% to 0.5% (v/v)). The calcein signal is normalized with respect to the calcein signal from cells not exposed to Tween 20. As shown, the background signal for the DMF assay was much lower than that from the well plate assay. As a consequence, the DMF results showed a >10 fold difference in the lethal concentration of Tween 20 (0.3%–0.5%) compared to the well plate results (0.03%–0.05%). Each point represents 4–6 replicates, and error bars are 1 SD.

15-fold; this is important, as cytotoxicity is widely used by regulatory agencies in initial screens for determining acceptable exposure limits, and by the pharmaceutical industry in early drug discovery.

Another cause of the improved sensitivity in droplet-based assays is the high cell concentration in ~nL droplets. The same number of cells in μL aliquots results in a much lower concentration and therefore, lower signal-to-noise ratio. In this experiment, 525 cells yielded 1.2×10^6 cells/mL in droplets, but only 3.5×10^4 cells mL^{-1} in wells. In addition, the cross-sectional density of cells in droplets was higher because of the slightly smaller droplet diameter (~1.8 mm) relative to that of the conical wells (2 mm bottom, 3.3 mm top). If it is assumed that all cells settled to the bottom of each well or droplet, then the same number of cells was distributed over an area that was ~20% smaller in droplets relative to wells, resulting in a higher signal. It is possible that all cells settled in droplets (150 μm height), while not all cells settled in wells (~5 mm height). If this were the case, it would obviously contribute to the observed differences in detection limits.

The results described above demonstrate that DMF can be used to implement cell-based assays with very high performance. With reduced reagent and cell consumption, and automated liquid manipulation, DMF devices outperformed standard well plate assays, and resulted in significant improvements in assay sensitivity. These data suggest great potential of DMF cell-based assays for phenotypic screening. In continuing work, we are developing DMF devices and methods capable of analyses of multiple cell samples in parallel, which should highlight these advantages further by application to high-throughput screening.

Conclusion

We have shown that digital microfluidics is a suitable technology for implementing cell-based assays. Cell suspensions at very high concentrations (>10 million mL^{-1}) were actuated with ease, and no significant difference in cell viability and proliferation after DMF actuation was observed. In addition, analysis of protein contents using mass spectrometry suggested that there are no major effects of actuation on cell biochemistry. To demonstrate the potential of DMF for implementing cell-based analyses, a cytotoxicity assay was performed. In this test, the digital microfluidic format outperformed an identical assay in a well plate, yielding 30× lower reagent consumption and a ~20-fold increase in sensitivity. The capacity to manipulate very small volumes and high cell/reagent concentrations makes digital microfluidics an attractive tool for cell-based assays, especially in cases in which reagents and cells are expensive and/or are available in limited quantities (*e.g.*, stem cells). The work reported here suggests great potential for the application of digital microfluidics to multiplexed phenotypic cell-based assays, an important tool used in drug discovery and environmental monitoring.

Acknowledgements

We thank Mohamed Abdelgawad for assistance with mask design and numerical simulations. We acknowledge the Natural Sciences and Engineering Council (NSERC) and the Canada Foundation for Innovation (CFI) for financial support. IBN thanks NSERC for a graduate fellowship, and ARW thanks the CRC for a Canada Research Chair.

References

1 A. S. Verkman, Drug Discovery in Academia, *Am. J. Physiol.: Cell Physiol.*, 2004, **286**, C465–C474.
2 J. El-Ali, P. K. Sorger and K. F. Jensen, Cells on Chips, *Nature*, 2006, **442**, 403–411.
3 S. K. W. Dertinger, D. T. Chiu, N. L. Jeon and G. M. Whitesides, Generation of Gradients Having Complex Shapes Using Microfluidic Networks, *Anal. Chem.*, 2001, **73**, 1240–1246.
4 N. Ye, J. Qin, W. Shi, X. Liu and B. Lin, Cell-Based High Content Screening Using an Integrated Microfluidic Device, *Lab Chip*, 2007, **7**, 1696–1704.
5 S. Takayama, E. Ostuni, P. LeDuc, K. Naruse, D. E. Ingber and G. M. Whitesides, Subcellular Positioning of Small Molecules, *Nature*, 2001, **411**, 1016–1016.
6 J. Kruger, K. Singh, A. O'Neill, C. Jackson, A. Morrison and P. O'Brien, Development of a Microfluidic Device for Fluorescence Activated Cell Sorting, *J. Micromech. Microeng.*, 2002, **12**, 486–494.
7 A. Y. Fu, H. P. Chou, C. Spence, F. H. Arnold and S. R. Quake, An Integrated Microfabricated Cell Sorter, *Anal. Chem.*, 2002, **74**, 2451–2457.
8 P. C. Li and D. J. Harrison, Transport, Manipulation, and Reaction of Biological Cells on-Chip Using Electrokinetic Effects, *Anal. Chem.*, 1997, **69**, 1564–1568.
9 E. A. Schilling, A. E. Kamholz and P. Yager, Cell Lysis and Protein Extraction in a Microfluidic Device with Detection by a Fluorogenic Enzyme Assay, *Anal. Chem.*, 2002, **74**, 1798–1804.
10 M. A. McClain, C. T. Culbertson, S. C. Jacobson, N. L. Allbritton, C. E. Sims and J. M. Ramsey, Microfluidic Devices for the High-Throughput Chemical Analysis of Cells, *Anal. Chem.*, 2003, **75**, 5646–5655.
11 A. R. Wheeler, W. Throndset, R. J. Whelan, A. M. Leach, R. N. Zare, Y.-H. Liau, K. Farrell, I. Manger and A. Daridon, Microfluidic Device for Single Cell Analysis, *Anal. Chem.*, 2003, **75**, 3581–3586.
12 J. G. Shackman, G. M. Dahlgren, J. L. Peters and R. T. Kennedy, Perfusion and Chemical Monitoring of Living Cells on a Microfluidic Chip, *Lab Chip*, 2005, **5**, 56–63.
13 M. J. Moehlenbrock, A. K. Price and R. S. Martin, Use of Microchip-Based Hydrodynamic Focusing to Measure the Deformation-Induced Release of ATP from Erythrocytes, *Analyst*, 2006, **131**, 930–937.
14 N. L. Jeon, H. Baskaran, S. K. W. Dertinger, G. M. Whitesides, L. Van De Water and M. Toner, Neutrophil Chemotaxis in Linear and Complex Gradients of Interleukin-8 Formed in a Microfabricated Device, *Nat. Biotechnol.*, 2002, **20**, 826–830.
15 B. Yap and R. D. Kamm, Mechanical Deformation of Neutrophils into Narrow Channels Induces Pseudopod Projection and Changes in Biomechanical Properties, *J. Appl. Physiol.*, 2005, **98**, 1930–1939.
16 B. D. DeBusschere and G. T. A. Kovacs, Portable Cell-Based Biosensor System Using Integrated CMOS Cell-Cartridges, *Biosens. Bioelectron.*, 2001, **16**, 543–556.
17 F. Morin, N. Nishimura, L. Griscom, B. LePioufle, H. Fujita, Y. Takamura and E. Tamiya, Constraining the Connectivity of Neuronal Networks Cultured on Microelectrode Arrays with Microfluidic Techniques: A Step Towards Neuron-Based Functional Chips, *Biosens. Bioelectron.*, 2006, **21**, 1093–1100.
18 T. Thorsen, S. J. Maerkl and S. R. Quake, Microfluidic Large-Scale Integration, *Science*, 2002, **298**, 580–584.
19 V. I. Chin, P. Taupin, S. Sanga, J. Scheel, F. H. Gage and S. N. Bhatia, Microfabricated Platform for Studying Stem Cell Fates, *Biotechnol. Bioeng.*, 2004, **88**, 399–415.
20 P. J. Hung, P. J. Lee, P. Sabounchi, R. Lin and L. P. Lee, Continuous Perfusion Microfluidic Cell Culture Array for High-Throughput Cell-Based Assays, *Biotechnol. Bioeng.*, 2005, **89**, 1–8.
21 Z. H. Wang, M. C. Kim, M. Marquez and T. Thorsen, High-Density Microfluidic Arrays for Cell Cytotoxicity Analysis, *Lab Chip*, 2007, **7**, 740–745.
22 M. A. Unger, H. P. Chou, T. Thorsen, A. Scherer and S. R. Quake, Monolithic Microfabricated Valves and Pumps by Multilayer Soft Lithography, *Science*, 2000, **288**, 113–116.

23 D. J. Beebe, J. S. Moore, J. M. Bauer, Q. Yu, R. H. Liu, C. Devadoss and B. H. Jo, Functional Hydrogel Structures for Autonomous Flow Control inside Microfluidic Networks, *Nature*, 2000, **404**, 588–590.
24 H. M. Yu, C. M. Alexander and D. J. Beebe, A Plate Reader-Compatible Microchannel Array for Cell Biology Assays, *Lab Chip*, 2007, **7**, 388–391.
25 J. Lee, H. Moon, J. Fowler, T. Schoellhammer and C.-J. Kim, Electrowetting and Electrowetting-on-Dielectric for Microscale Liquid Handling, *Sens. Actuators, A*, 2002, **95**, 259–268.
26 M. G. Pollack, R. B. Fair and A. D. Shenderov, Electrowetting-Based Actuation of Liquid Droplets for Microfluidic Applications, *Appl. Phys. Lett.*, 2000, **77**, 1725–1726.
27 T. B. Jones, K. L. Wang and D. J. Yao, Frequency-Dependent Electromechanics of Aqueous Liquids: Electrowetting and Dielectrophoresis, *Langmuir*, 2004, **20**, 2813–2818.
28 O. D. Velev, B. G. Prevo and K. H. Bhatt, On-Chip Manipulation of Free Droplets, *Nature*, 2003, **426**, 515–516.
29 J. A. Schwartz, J. V. Vykoukal and P. R. C. Gascoyne, Droplet-Based Chemistry on a Programmable Micro-Chip, *Lab Chip*, 2004, **4**, 11–17.
30 R. Mukhopadhyay, Diving into Droplets, *Anal. Chem.*, 2006, **78**, 1401–1404.
31 T. Taniguchi, T. Torii and T. Higuchi, Chemical Reactions in Microdroplets by Electrostatic Manipulation of Droplets in Liquid Media, *Lab Chip*, 2002, **2**, 19–23.
32 V. Srinivasan, V. K. Pamula and R. B. Fair, Droplet-Based Microfluidic Lab-on-a-Chip for Glucose Detection, *Anal. Chim. Acta*, 2004, **507**, 145–150.
33 V. Srinivasan, V. K. Pamula and R. B. Fair, An Integrated Digital Microfluidic Lab-on-a-Chip for Clinical Diagnostics on Human Physiological Fluids, *Lab Chip*, 2004, **4**, 310–315.
34 D. Jary, A. Chollat-Namy Fouillet, Y. J. Boutet, C. Chabrol, G. Castellan, D. Gasparutto and C. Peponnet, DNA Repair Enzyme Analysis on EWOD Fluidic Microprocessor, in *Proceedings of the NSTI Nanotechnology Conference and Trade Show Nanotech*, 2006, vol. 2, pp. 554–557.
35 E. M. Miller and A. R. Wheeler, A Digital Microfluidic Approach to Homogeneous Enzyme Assays, *Anal. Chem.*, 2008, **80**, 1614–1619.
36 A. R. Wheeler, H. Moon, C.-J. Kim, J. A. Loo and R. L. Garrell, Electrowetting-Based Microfluidics for Analysis of Peptides and Proteins by Matrix Assisted Laser Desorption/Ionization Mass Spectrometry (MALDI-MS), *Anal. Chem.*, 2004, **76**, 4833–4838.
37 A. R. Wheeler, H. Moon, C. A. Bird, R. R. O. Loo, C.-J. Kim, J. A. Loo and R. L. Garrell, Digital Microfluidics with in-Line Sample Purification for Proteomics Analyses with MALDI-MS, *Anal. Chem.*, 2005, **77**, 534–540.
38 H. Moon, A. R. Wheeler, R. L. Garrell, J. A. Loo and C. J. Kim, An Integrated Digital Microfluidic Chip for Multiplexed Proteomic Sample Preparation and Analysis by MALDI-MS, *Lab Chip*, 2006, **6**, 1213–1219.
39 Y. H. Chang, G. B. Lee, F. C. Huang, Y. Y. Chen and J. L. Lin, Integrated Polymerase Chain Reaction Chips Utilizing Digital Microfluidics, *Biomed. Microdevices*, 2006, **8**, 215–225.
40 P. W. Huang, T. T. Wang, S. W. Lin, Y. C. Chang and S. K. Fan, Dielectrophoretic Cell Concentrator on EWOD-Based Chips, in *Proceedings of the 1st IEEE International Conference on Nano/Micro Engineered and Molecular Systems*, 2006, pp. 1418–1421.
41 D. Chatterjee, B. Hetayothin, A. R. Wheeler, D. J. King and R. L. Garrell, Droplet-Based Microfluidics with Nonaqueous Solvents and Solutions, *Lab Chip*, 2006, **6**, 199–206.
42 J. Y. Yoon and R. L. Garrell, Preventing Biomolecular Adsorption in Electrowetting-Based Biofluidic Chips, *Anal. Chem.*, 2003, **75**, 5097–5102.
43 M. Amiji and K. Park, Prevention of Protein Adsorption and Platelet-Adhesion on Surfaces by PEO PPO PEO Triblock Copolymers, *Biomaterials*, 1992, **13**, 682–692.
44 C. M. Smith, R. P. Hebbel, D. P. Tukey, C. C. Clawson, J. G. White and G. M. Vercellotti, Pluronic F-68 Reduces the Endothelial Adherence and Improves the Rheology of Liganded Sickle Erythrocytes, *Blood*, 1987, **69**, 1631–1636.
45 A. Mizrahi, Pluronic Polyols in Human Lymphocyte Cell Line Cultures, *J. Clin. Microbiol.*, 1975, **2**, 11–13.
46 Hyclone Media: Cho Cell Culture Platform Media, http://www.hyclone.com/media/cho.htm, accessed on November 10, 2007.
47 V. N. Luk, G. C. H. Mo and A. R. Wheeler, Pluronic Additives: A Solution to Sticky Problems in Digital Microfluidics, *Langmuir*, 2008, submitted.
48 B. Thiede, F. Siejak, C. Dimmler, P. R. Jungblut and T. Rudel, A Two Dimensional Electrophoresis Database of a Human Jurkat T-Cell Line, *Electrophoresis*, 2000, **21**, 2713–2720.

